Synthesis and magnetic properties of gold coated iron oxide nanoparticles

Susmita Pal, Marienette Morales, Pritish Mukherjee, and Hariharan Srikanth[a)]
Center for Integrated Functional Materials and Department of Physics, University of South Florida, Tampa, 33620 Florida, USA

(Presented 13 November 2008; received 15 September 2008; accepted 22 October 2008; published online 5 February 2009)

We report on synthesis, structural, and magnetic properties of chemically synthesized iron oxide (Fe_3O_4) and Fe_3O_4@Au core-shell nanoparticles. Structural characterization was done using x-ray diffraction and transmission electron microscopy, and the magnetite phase of the core (~6 nm) and fcc Au shell (thickness of ~1 nm) were confirmed. Magnetization (M) versus temperature (T) data at $H=200$ Oe for zero-field-cooled and field-cooled modes exhibited a superparamagnetic blocking temperature $T_B \sim 35$ K (40 K) for parent (core-shell) system. Enhanced coercivity ($H_c \sim 200$ Oe) at 5 K along with nonsaturating M-H loops observed for Fe_3O_4@Au nanoparticles indicate the possible role of spin disorder at the Au–Fe_3O_4 interface and weak exchange coupling between surface and core spins. Analysis of ac susceptibility (χ' and χ'') data shows that the interparticle interaction is reduced upon Au coating and the relaxation mechanism follows the Vogel–Fulcher law. © *2009 American Institute of Physics*. [DOI: 10.1063/1.3059607]

Layered assembly of different materials in core-shell nanoparticle (NP) form is an attractive way to fabricate systems possessing diverse physical and chemical properties.[1–4] Multicomponent NPs exhibit distinct optical,[5,6] catalytic,[7] and magnetic[8] properties. Recently, incorporation of optically active components onto magnetic NPs has attracted considerable attention. Gold (Au) coated superparamagnetic NPs are very attractive composite systems.[9,10] Dumbbell-like Au–Fe_3O_4 (Refs. 3 and 11) and CdS–FePt (Ref. 12) NPs have been synthesized and exhibit interesting optical properties (due to Au or CdS) and magnetic properties (due to Fe_3O_4 or FePt). One of the drawbacks in these composite systems is that the magnetic moment decreases considerably, which is a major constraint for biomedical applications. This can originate from several sources such as interface coupling, nonmagnetic surface layer, reduction in interparticle interactions, etc. In this study, we report on the synthesis, structure, and magnetic characterization of nearly spherical iron oxide NPs ($D \sim 6$ nm) and its gold-coated counterpart, with shell thickness of Au of about 1 nm.

The Fe_3O_4 NPs capped with oleylamine and oleic acid were synthesized using a chemical procedure reported elsewhere.[13] In a typical synthesis process, 10 mmol 1,2-hexadecanediol, 6 mmol oleic cid, 6 mmol oleylamine, and 20 ml benzyl ether were added to 2 mmol iron (III) acetylacetonate. The mixture was heated to 200 °C for 2 h with constant stirring and then refluxed at ~300 °C for another 1 h in the presence of argon. Then 40 ml ethanol was added to the cooled mixture and a black precipitate was separated by centrifugation. The black product was dissolved in hexane in the presence of oleic acid (~0.05 ml) and oleylamine (~0.05 ml) and centrifuged to remove the undispersed residue. The product of 6 nm Fe_3O_4 particles was then precipitated with ethanol, centrifuged to remove the solvent, and redispersed into hexane. The synthesis of Au-coated Fe_3O_4 NPs was followed by an initial synthesis of Fe_3O_4 NPs as seeds and a subsequent reduction in gold acetate [$Au(OOCCH_3)_3$] in the presence of the seeds.

Figure 1 shows a representative set of transmission electron microscopy (TEM) micrographs of Fe_3O_4 nanoparticles before and after the formation of the gold shell. Histograms (not shown) of the particle size distribution from the TEM images with a sampling of 50 particles were analyzed, and this yielded mean particle sizes of 6 nm for particles before coating [Fig. 1(a)] and 7 nm for the particles after coating [Fig. 1(b)] with Au.

The x-ray diffraction (XRD) patterns of parent and Au-coated Fe_3O_4 NPs exhibit the diffraction peaks for inverse spinel ferrite structure and fcc phase of gold, respectively, as

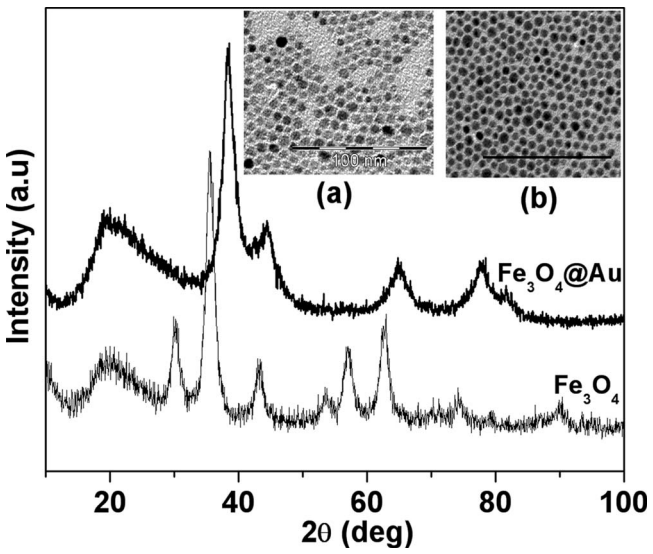

FIG. 1. XRD pattern of as-synthesized Fe_3O_4 and Fe_3O_4@Au NPs. Shown in the inset are TEM pictures of (a) Fe_3O_4 and (b) Fe_3O_4@Au NPs.

[a)]Author to whom correspondence should be addressed. Electronic mail: sharihar@cas.usf.edu.

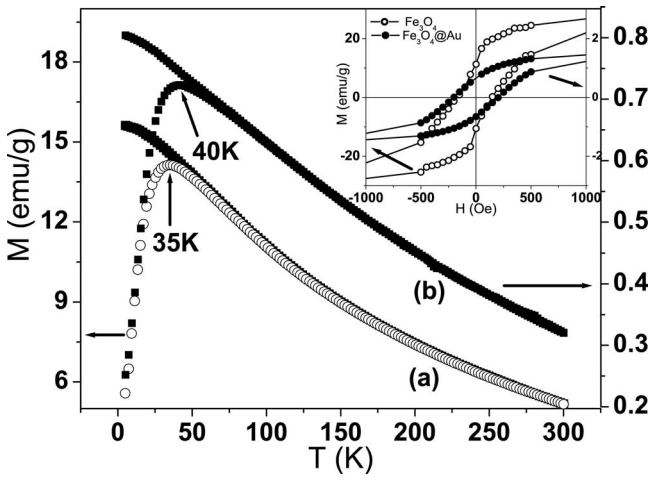

FIG. 2. Magnetization vs temperature plot (T=5 K) at H=200 Oe of (a) Fe_3O_4 and (b) Fe_3O_4@Au NPs. Inset figure shows the hysteresis loop (T=5 K) of Fe_3O_4 (-○-) and Fe_3O_4@Au (-●-) NPs.

shown in Fig. 1. The absence of the diffraction peaks for Fe_3O_4 phase in Fe_3O_4@Au NPs is a strong evidence for complete coverage of the iron oxide core by the gold shell. This is most likely due to the heavy atom effect of gold compared to iron oxide.[14]

Temperature and field dependent DC and AC magnetization along with radio frequency (RF) transverse susceptibility were done in a commercial physical properties measurement system from Quantum Design. The M vs T data measured at H=200 Oe in ZFC-FC modes for the Fe_3O_4 and Fe_3O_4@Au NPs exhibit a characteristic superparamagnetic response at high T with blocking temperature (T_B) around 35 and 40 K, respectively, as shown in Fig. 2. The slight increase in blocking temperature for Au-coated particles can be due to the overall increase in particle size as observed from TEM. M vs H was measured at applied fields of ±50 kOe at 5 K under ZFC-FC modes. The saturation magnetization M_s of Fe_3O_4 NPs and Fe_3O_4@Au are estimated to be 33 and 1.8 emu/g, respectively, which are significantly lower than that of bulk Fe_3O_4 (M_s=84 emu/g). This reduction is expected in NPs as the surface magnetic order can be affected by structural distortions that cause spin canting.[15] The drastically reduced moment in Fe_3O_4@Au NPs indicates that the contribution of surface effects should be significantly higher when compared with uncoated Fe_3O_4. M-H loops did not exhibit hysteresis in the superparamagnetic state for both the parent Fe_3O_4 and Fe_3O_4@Au NPs as expected, and at T=5 K within the blocked state, the measured coercivities were H_c=160 and 200 Oe, respectively (insets of Fig. 2). We also measured the M-H loops after field cooling to 5 K to look for any possible exchange bias that could result in coercivity enhancement. However, the loops were symmetric and no exchange bias was found for both particle systems.

The temperature-dependent (5–150 K) ac susceptibility [both in phase $\chi'(T)$ and out of phase $\chi''(T)$] was measured over the frequency window from 10 Hz to 10 kHz for both uncoated and Au-coated samples (Figs. 3 and 4). The magnetic relaxation of noninteracting NPs is expected to follow the thermally activated Néel–Arrhenius law given by the expression $f=f_0\exp(-E_a/k_BT_B)$, where f_0 (attempt frequency)

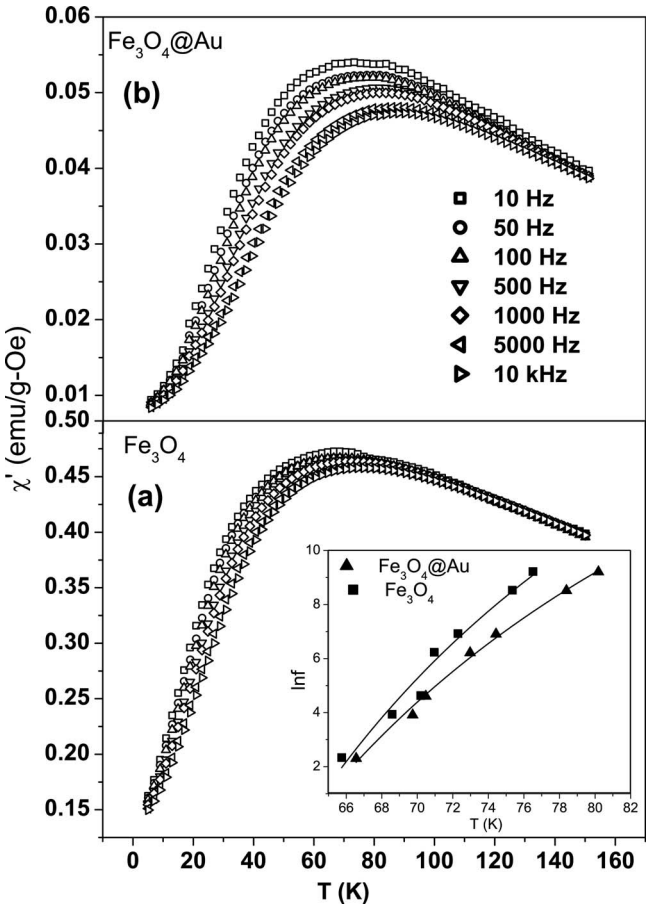

FIG. 3. Temperature dependence of ac susceptibility χ' (in phase) of (a) Fe_3O_4 and (b) Fe_3O_4@Au NPs for several frequencies. The inset shows the fitting of Vogel–Fulcher relaxation mechanism for both samples.

is of the order of 10^9-10^{13} Hz, k_B is Boltzmann's constant, and E_a is the anisotropy energy. In the case of weakly interacting NPs, the system is expected to conform to the framework of the Vogel–Fulcher relaxation: $f=f_0\exp[-E_a/k_B(T_B-T_0)]$ with T_0 as the effective strength of interparticle interactions. As expected from these expressions, the blocking temperature increases with increasing frequency. It is clearly seen that the T_B shifts to a slightly higher value in Fe_3O_4@Au compared to the uncoated Fe_3O_4 NPs, which also supports the dc magnetization (M vs T) results. Fits to the Néel–Arrhenius model yields unphysical values for f_0 (10^{20} Hz), whereas reasonable values for f_0 are obtained from fits to the Vogel–Fulcher relation.[16] The fit values of f_0, E_a/k_B, and T_0 for the uncoated (coated) particles are 5.0×10^{13} (5.0×10^{12}) Hz, 1003 (1042) K, and 32 (28) K, respectively, and the plots are shown in the inset of Fig. 3. These parameters extracted from the fits suggest that the interparticle interaction is reduced a bit in gold-coated NPs. We have also analyzed the $\chi''(T)$ vs T data using a phenomenological relation:[17]

$$\Phi = \Delta T_p/T_p\Delta \log_{10} f,$$

where ΔT_p is the shift in peak temperature T_p observed in the frequency interval $\Delta \log_{10} f$. It has been shown from a number of experimental observations that the numerical value of $\Phi>0.1$ for noninteracting NPs, Φ=0.03–0.1 for interacting

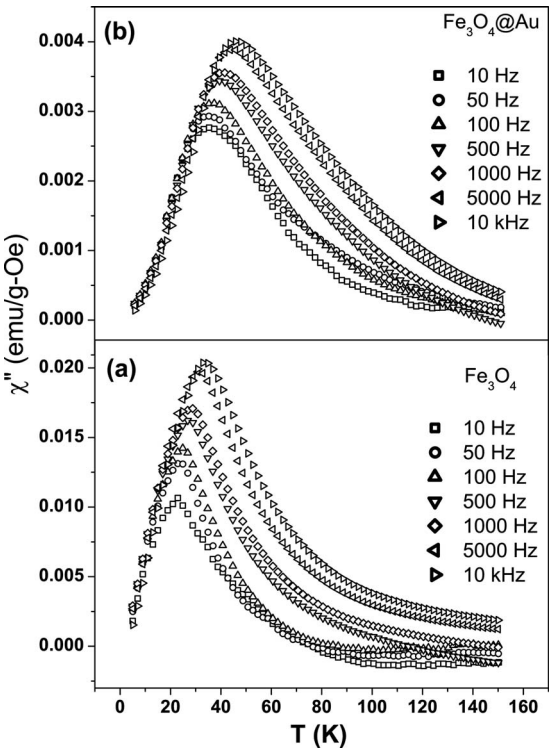

FIG. 4. Temperature dependence of ac susceptibility χ'' (out of phase) of (a) Fe_3O_4 and (b) Fe_3O_4@Au NPs for several frequencies.

NPs, and $\Phi < 0.03$ for spin-glass system.[18] Our experimental result gives the Φ values of 0.07 (0.1) for the uncoated (coated) samples. These results again confirm that the gold shells on iron oxide cores encapsulate and shield the magnetic particles and cause a reduction in the overall interparticle magnetic interaction.

Over the years, we have pioneered the method of rf TS as a powerful method for directly probing the effective magnetic anisotropy in nanoparticle systems.[19,20] Field-dependent TS data for field scans of ±10 kOe were collected over a temperature range 10 K $< T <$ 300 K for both the uncoated and Au-coated NP systems (Fig. 5). The two peaks corresponding to the anisotropy field ($\pm H_k$) were observed below blocking temperature and the peaks merge into a single peak at $H=0$ above blocking temperature, consistent with earlier studies on NP samples.[19,20] At $T=10$ K, the anisotropy field is around 450 Oe, which is in the range of values (250–500 Oe) typically observed in Fe_3O_4 NPs. The effective anisotropy is determined by various factors such as particle size, shape, interparticle interactions, and surface/core spin ordering. The inset of Fig. 5 shows the temperature dependence of $\pm H_k$ values for both Fe_3O_4 and Fe_3O_4@Au. The values are similar, indicating that the thin Au shell in these NPs with nearly spherical symmetry do not significantly change the effective anisotropy. However, we note that the relative magnitude of TS decreases an order of magnitude in the gold-coated sample, consistent with the large reduction in magnetic moment.

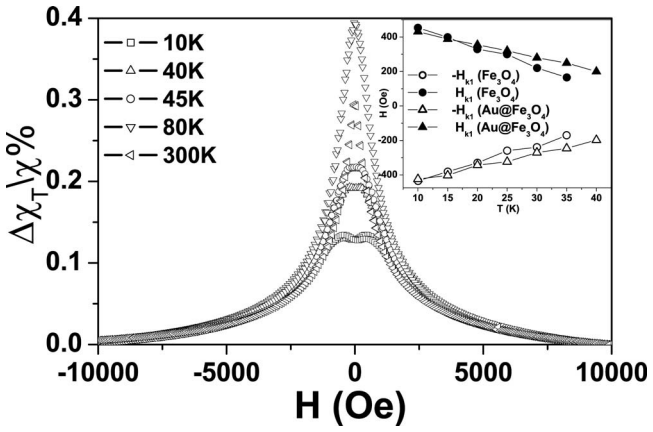

FIG. 5. TS measurement of the Fe_3O_4@Au NPs. Inset figure shows temperature dependence of H_k for both the coated and uncoated NPs.

This work is supported by DoD-USAMRMC through Grant No. W81XWH-07-1-0708. The authors thank Manh-Huong Phan, Natalie Frey, and Melody Miner for useful discussions and assistance with experiments.

[1]D. J. Milliron, S. M. Hughes, Y. Cui, L. Manna, J. B. Li, L. W. Wang, and A. P. Alivisatos, Nature (London) **430**, 190 (2004).
[2]H. W. Gu, R. K. Zheng, X. X. Zhang, and B. Xu, J. Am. Chem. Soc. **126**, 5664 (2004).
[3]H. Yu, M. Chen, P. M. Rice, S. X. Wang, R. L. White, and S. Sun, Nano Lett. **5**, 379 (2005).
[4]R. D. Robonson, B. Sadtler, D. Demchenko, C. K. Erdonmez, L.-W. Wang, and A. P. Alivisatos, Science **317**, 355 (2007).
[5]H. Kim, M. Achermann, L. P. Ballet, J. A. Hollingsworth, and V. I. Klimov, J. Am. Chem. Soc. **127**, 544 (2005).
[6]J. K. Lim, A. Eggeman, F. Lenni, R. D. Tilton, and S. A. Majetich, Adv. Mater. (Weinheim, Ger.) **20**, 1721 (2008).
[7]J. W. Yoo, D. Hathcock, and M. A. El-Sayed, J. Phys. Chem. A **106**, 2049 (2002).
[8]L. Wang, H.-Y. Park, S. I.-I. Lim, M. J. Schadt, D. Mott, J. Luo, X. Wang, and C.-J. Zhong, J. Mater. Chem. **18**, 2629 (2008).
[9]J. Lin, W. Zhou, A. Kumbhar, J. Wiemann, J. Fang, E. E. Carpenter, and C. J. O'Connor, J. Solid State Chem. **159**, 26 (2001); J. L. Lyon, D. A. Fleming, M. B. Stone, P. Schiffer, and M. E. Williams, Nano Lett. **4**, 719 (2004).
[10]L. Y. Wang, J. Luo, Q. Fan, M. Suzuki, I. S. Suzuki, M. H. Engelhard, Y. H. Lin, N. Kim, J. Q. Wang, and C. J. Zhong, J. Phys. Chem. B **109**, 21593 (2005).
[11]N. A. Frey, S. Srinath, H. Srikanth, T. Chao, and S. Sun, IEEE Trans. Magn. **43**, 3094 (2007).
[12]H. W. Gu, R. K. Zheng, X. X. Zhang, and B. Xu, J. Am. Chem. Soc. **126**, 5664 (2004); H. W. Gu, Z. M. Yang, J. H. Gao, C. K. Chang, and B. Xu, J. Am. Chem. Soc. **27**, 34 (2005).
[13]S. Sun and H. Zheng, J. Am. Chem. Soc. **124**, 8204 (2004).
[14]M. F. C. Ladd and R. A. Palmer, *Structure determination by x-ray crystallography*, 3rd ed. (Plenum, New York, London, 1993).
[15]M. P. Morales, S. Veintemillas-Verdaguer, M. I. Montero, C. J. Serna, A. Roig, L1. Casas, B. Martinez, and F. Sandiumenge, Chem. Mater. **11**, 3058 (1999).
[16]S. Shtrikman, and E. P. Wohlfarth, Phys. Lett. **85A**, 467 (1981).
[17]J. Dormann, Phys. Rev. B **53**, 14291 (1996).
[18]G. F. Goya, T. S. Berquó, F. C. Fonseca, and M. P. Morales, J. Appl. Phys. **94**, 3520 (2003) and references therein.
[19]P. Poddar, J. L. Wilson, H. Srikanth, D. F. Farrell, and S. A. Majetich, Phys. Rev. B **68**, 214409 (2003).
[20]P. Poddar, H. Srikanth, S. A. Morrison, and E. E. Carpenter, J. Magn. Magn. Mater. **288C**, 443 (2005).